Complete Wetting on a Linear Wedge

L. Bruschi, A. Carlin, and G. Mistura

Istituto Nazionale per la Fisica della Materia and Dipartimento di Fisica G. Galilei, Università di Padova, via Marzolo 8, 35131 Padova, Italy

(Received 10 April 2002; published 30 September 2002)

We have measured the growth of liquid films of Ar adsorbed on well defined arrays of microscopic linear wedges sculpted on thin Si wafers and on a stainless steel disk. On these patterns, a clear crossover from a planarlike to a geometry dependent growth behavior is observed. This crossover is found to depend on the characteristic wedge size. Near liquid-vapor bulk coexistence, the film mass is observed to diverge as a power law of the chemical potential difference from saturation with an exponent in very good agreement with the value of -2 expected for a linear wedge. This exponent is not affected by the opening angles of the wedges. All these findings are in accordance with a recent scaling theory.

DOI: 10.1103/PhysRevLett.89.166101 PACS numbers: 68.08.Bc, 64.70.Fx, 68.35.Md

It is well known that the growth of an adsorbed film is strongly affected by the geometry of the substrate. On a flat surface, the growth parameters depend only on the physical interactions between adsorbate-substrate and adsorbate-adsorbate. In all other cases, there is a rich interplay between physics and geometry. For example, by means of adsorption measurements, it is possible to derive the fractal dimension of a rough substrate [1] produced by evaporation or erosion. If a liquid film is instead adsorbed in a porous medium, a complex phenomenology is observed that depends on the pore size distribution and connectivity [2]. More recently, increasing research efforts have been devoted to patterned substrates [3] given their potentially relevant applications in as diverse fields as biophysics [4] and microfluidics [5]. Computer simulations suggest that patterned substrates also drastically influence the nature of surface freezing [6]. At the same time, the study of the wetting behavior of liquid films in wedges has shown a rich variety of novel phase transitions that are extremely sensitive to the shape of the confining geometry [7].

This work is concerned with the growth of a liquid film adsorbed on a linear wedge formed by joining two oblique planes. Wetting on an oblique corner was first studied as a simplified example of the geometry of a porous medium [8] and then because of its strong influence on the growth of an adsorbed liquid film [9,10]. The film growth in a linear wedge can be derived by simple stability conditions [9] in the case of complete wetting at coexistence, that is, when the liquid film covers uniformly the wedge walls. At a given undersaturation $-\delta\mu \equiv \mu_0 - \mu$, where μ_0 represents the chemical potential of the vapor in equilibrium with the film at liquid-vapor bulk coexistence and μ represents that corresponding to a certain pressure P of the vapor, the radius of curvature of the meniscus separating the liquid confined at the bottom of the wedge from its vapor is given by the Laplace equation [11]. If the liquid completely wets the surface walls, the film profile should become parallel to the wedge walls at a certain distance from the wedge bottom. Simple trigonometric considerations applied to this geometry then show that the excess mass m_l of a liquid adsorbed in a linear 3D wedge is expected to grow as $m_l \sim (-\delta\mu)^{-2}$ [9,12]. This behavior sharply contrasts with that observed on a flat surface where $m_l \sim (-\delta\mu)^{-1/3}$, if the liquid film is attracted to the surface by means of van der Waals forces [11].

The result on the linear wedge has been extended to power law wedges, whose height profiles have the form $h = A|y|^{\gamma}$, where A is a constant, y is the lateral coordinate measured from the bottom of the channel, and the exponent $\gamma > 0$ characterizes its curvature. According to recent scaling arguments [12], there exists a marginal value of the height exponent γ^* ($\gamma^* = 1/2$ for van der Waals forces) such that for $\gamma > \gamma^*$ a crossover from planarlike to geometry dependent behavior is expected, whose location depends on the size of the channels. In this latter regime, $m_l \sim (-\delta\mu)^x$, where $x = \frac{\gamma+1}{\gamma-2}$ and $\gamma^* < \gamma \leq 1$. An interesting conclusion of this theory is that the exponent x depends only on γ. For a linear wedge, $\gamma = 1$, this implies that the resulting exponent x must be equal to -2 no matter how wide the opening angle α of the wedge is.

We have thus decided to test these predictions in the laboratory by using two different substrates. The first one is formed by two squared pieces of Si (side 1 cm and thickness 300 μm), which have been patterned by wet chemical etching on both faces [13]. The resulting pattern is a regular array of parallel linear wedges with an opening angle of 75° and a depth of 1.3 μm. Two consecutive channels are separated by a flat stripe 2 μm wide. Figure 1 displays two micrographs of this pattern obtained with the electron microscope.

We have also analyzed this structure with an atomic force microscope. Typical scans of the silicon surface taken along paths transverse to the channels are displayed in the top part of Fig. 2. The results of this study indicate that the Si surface has an rms roughness ≤ 15 Å.

The second substrate is a thin stainless steel (s.s.) disk, diameter 2 cm and thickness 300 μm, whose faces have

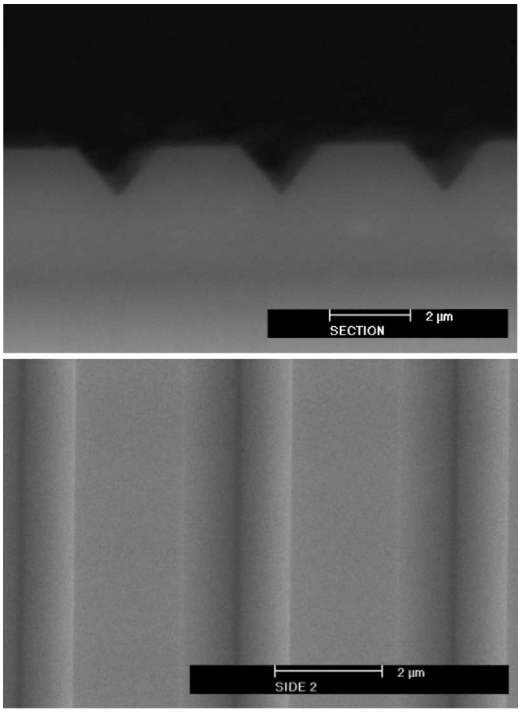

FIG. 1. Cross section and top view of the silicon patterned surface taken with the electron microscope.

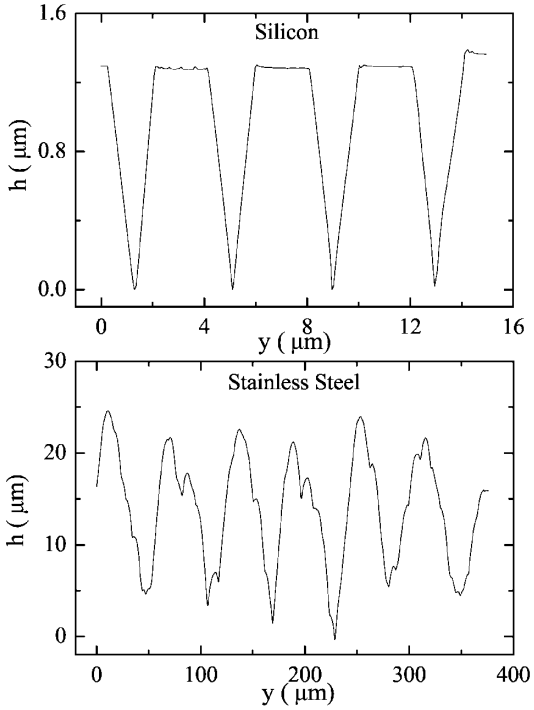

FIG. 2. Top: AFM scans measured across the channels. Bottom: Profile of the s.s. disk measured with a profile meter. Note the different scales.

been patterned by laser ablation that produces deep, concentric channels. The bottom of Fig. 2 shows the resulting pattern measured with the profile meter. It is characterized by an almost periodic array of triangular channels with a typical opening angle of 110° ± 10%, which are much deeper ($\sim 20\ \mu$m) and wider ($\sim 60\ \mu$m) than those sculpted on silicon.

The samples are epoxied to the extremity of a hardened steel rod and are driven to the torsional resonant frequency of the system:

$$\nu = \frac{1}{2\pi}\sqrt{\frac{K}{I}}, \tag{1}$$

where K is the elastic constant and I is the total moment of inertia. A schematic drawing of the torsional disk oscillator used in our measurements is shown in the inset of Fig. 3. The top view B refers to the Si square wafers and that of C to the s.s. disk. As the substrate is exposed to a gas of density ρ and viscosity η, the resonance frequency changes because of a variation of the moment of inertia. If I_0 and ν_0 indicate the moment of inertia and the resonance frequency in vacuum, the change ΔI of the moment of inertia will be given, from Eq. (1), by

$$\frac{\Delta I}{I_0} = \left(\frac{\nu_0}{\nu}\right)^2 - 1 \approx 2\frac{(\nu_0 - \nu)}{\nu_0}, \tag{2}$$

where the linearization is justified by the small relative frequency change during the measurements (typically much less than 0.1%).

The relative increase $\Delta I/I_0$ is caused by the mass of the adsorbed film and by the hydrodynamic contribution due to the mass of the dynamically displaced fluid. For the two substrate geometries used in this study, the frequency decrease due to this viscous coupling V is expected to be a simple function of the vapor density and viscosity; that is, $V \equiv V(\sqrt{\pi\rho\eta\nu})$ [14,15]. We have evaluated the validity of this correction and determined the geometrical factors appearing in V by taking extensive vapor pressure adsorption isotherms of He, Ne, and Ar at

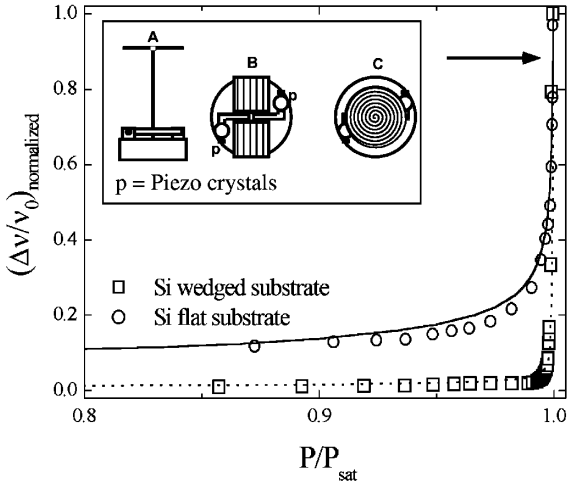

FIG. 3. Adsorption isotherms taken at 85 K on a patterned and on a flat Si substrate. The lines are the theoretical curves expected for a structured and for a flat surface. The inset gives a schematic view of the torsional oscillator setups. For more details, see text.

room temperature, where the only contribution to the frequency is due to the viscous coupling to the vapor. Finally, if we make the reasonable assumption that, in equilibrium conditions, a homogeneous film covers the substrate, then $\Delta I_{\rm film}/I_0$ is proportional to the film mass m_l. Therefore, apart from a multiplicative factor,

$$m_l \sim \frac{\nu_0 - \nu - V(\sqrt{\pi\rho\eta\nu})}{\nu_0} \equiv \frac{\nu_0 - \nu^*}{\nu_0}, \qquad (3)$$

where ν^* represents the vapor corrected oscillator frequency.

The torsional mode is excited by means of a small piezoelectric crystal acting onto the extremity of a stainless steel arm hard soldered to the torsion rod. The oscillations are detected by a similar piezo mounted in a symmetric way with respect to the other one. The induced voltage is amplified by a low noise homemade amplifier and a lock-in technique locks the electronic circuit onto the resonant frequency of the microbalance.

The microbalance is mounted inside a double wall copper cell to reduce thermal gradients [15] and is housed in the vacuum space of a homemade bath cryostat. To eliminate the pressure variations due to the daily oscillations in the temperature of the lab, we have placed the capacitance pressure gauge right before the cryostat. The open volume of the cell and of the sensor, which is kept at a constant temperature, can be sealed off from the gas system by means of a valve. In this way, the pressure reading is maintained stable within ± 0.05 Torr for periods of days.

With this setup we have measured the adsorption of Ar films at a constant temperature of 85 K, about 1 K above the bulk triple-point T_t (Ar is well known to completely wet Si and s.s. at coexistence at any $T > T_t$). Figure 3 shows the vapor corrected frequency shifts measured on the patterned Si as a function of the relative pressure $P/P_{\rm sat}$ of the gas in equilibrium with the film. For the sake of clarity, we have plotted only the final portion of the isotherm and the relative shifts have been normalized to the value of 6.63×10^{-4} observed at a relative pressure $P/P_{\rm sat} = 0.9996$.

The horizontal arrow marks the frequency calculated on the assumption that the wedges are perfectly filled with liquid argon up to their rim. This estimate is based on the determination of the moment of inertia of the substrate from its geometry and mass and ignores any curvature effect due to capillarity. The position of the arrow then suggests that the final point of the isotherm likely corresponds to a situation where the wedges are full and the flat stripes are covered with a thick liquid film.

In Fig. 3 we have also shown an Ar adsorption isotherm taken at the same temperature by using the same microbalance but with a flat substrate. This is realized with two thin, squared pieces of Si (side 0.9 cm and thickness 300 μm) epoxied to the torsion rod, which have been optically polished on both faces. Again, the data points have been scaled to the same geometric area of the wedged substrate and normalized to the relative frequency shift of 3.2×10^{-5} measured at $P/P_{\rm sat} = 0.9996$. This latter normalization is the reason why the isotherm on the flat surface lies above that on the patterned one. In reality, the saturated frequency shift measured on the wedged substrate is about 20 times larger than that on the flat silicon. The saturated film thickness observed on this latter substrate corresponds to about 150 Å.

Finally, to facilitate the data interpretation, we have plotted in the same graph the theoretical curve (dashed line) expected for the film growth on the structured silicon surface. If we ignore the very small crossover region linking the film on the flat region to that in the wedge, the mass loading of the microbalance is well approximated by [16]:

$$\frac{m_l}{m_{\rm Ar}} \sim \rho_l A\left(\frac{-\delta\mu}{H}\right)^{-1/3} + N_w L \frac{(\tan\alpha - \alpha)\sigma_{lv}^2}{(\rho_l - \rho_v)}(-\delta\mu)^{-2}, \qquad (4)$$

where $\rho_{l,v}$ represents the number density of liquid (vapor) Ar, A is the total surface area of the patterned Si, $H = 1.25$ eV Å^3 is the Hamacker constant between a Si surface and Ar [17], $N_w = 2500$ is the number of wedges of the substrate, L is the side of the Si square, $\alpha = 53°$ is the angle the wedge forms with the horizontal, σ_{lv} is the liquid-vapor surface tension of Ar, and $m_{\rm Ar}$ is the mass of an Ar atom.

The solid line represents instead the Frenckel-Halsey-Hill adsorption isotherm [term proportional to $(-\delta\mu)^{-1/3}$ in the above equation] calculated with the same Hamacker constant. We point out that these two curves are not fits to the data but simply the results of the mentioned formulas. On this scale, the agreement with the corresponding experimental points is quite good.

Two general qualitative conclusions can be already drawn from this comparison. First of all, the behavior observed with the polished Si is quite different from that we have measured with the structured Si attached to the same torsional oscillator, indicating that the latter is not an artifact of our technique. Second, the simple power law expected for a flat substrate does not describe at all the sharp divergence observed near liquid-vapor bulk coexistence on the patterned sample.

A more quantitative analysis of the experimental points has been done by plotting the logarithm of the vapor corrected frequency shifts close to saturation as a function of log $\ln(P_{\rm sat}/P)$, because for the chemical potential difference from saturation we have used the ideal gas formula, that is, $-\delta\mu = K_B T \ln(P_{\rm sat}/P)$. For a better comparison, we have used different horizontal and vertical scales for the two data sets. The horizontal error bars are related to the finite resolution of ± 0.05 Torr in the measurement of the vapor pressure. The solid lines represent the results of the linear fits to these extremities. The slopes of the lines corresponding to the flat silicon are

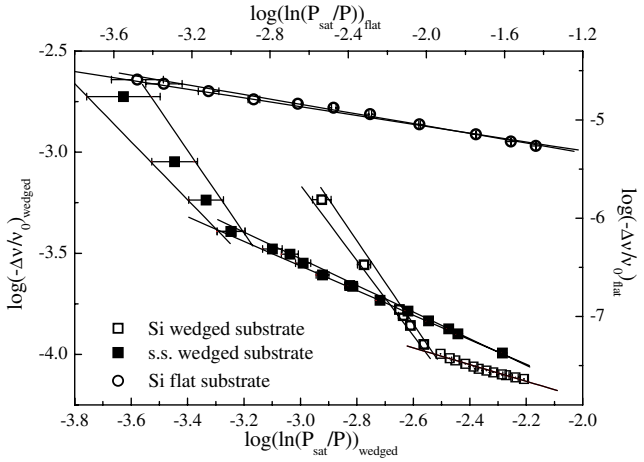

FIG. 4. Determination of the growth exponents of the liquid film of Ar adsorbed on the patterned substrates and on a flat one.

comprised between $x = -0.31$ and $x = -0.35$ as expected. We have also analyzed these data taking into account the virial correction to $-\delta\mu$ without finding any appreciable difference in the calculated exponents.

Instead, on the patterned Si, the adsorption isotherm clearly shows two distinct regimes: an initial growth characterized by an exponent $x = -0.35 \pm 0.01$ followed by a steeper increase near bulk-liquid vapor coexistence when the channels start to get filled with an exponent $x = -1.96 \pm 0.10$. In other words, there is a crossover from a planar to a geometrically dominated regime similar to that found numerically by Rascón and Parry in their mean field analysis of wedges of different shapes [12]. The exponent measured near saturation is in good agreement with the predicted value of -2 [9,12].

In the same graph, we have also plotted the final portion of an Ar adsorption isotherm measured at the same temperature but with the s.s. disk. Its behavior closely resembles that observed on the patterned Si. Again, there is an initial growth with an exponent $x = -0.6 \pm 0.05$ followed by a steeper increase very near saturation with an exponent $x = -1.8 \pm 0.25$. The discrepancy between the first exponent and the value of $-1/3$ expected on a flat surface is probably caused by the microscopic roughness (rms value $\sim$100 Å) of the s.s. sample produced by the laser ablation process. We have found similar variations of x with the substrate roughness in previous wetting studies on solid surfaces [18].

The exponent observed near P_{sat} is instead in agreement with the value expected for a linear wedge. In this case, the larger error bars are caused by the close vicinity to saturation. For instance, the final point of the s.s. isotherm in Fig. 4 refers to a pressure only 0.10 Torr less than $P_{\text{sat}} = 572.45$ Torr. The fact that even on this different pattern we get a growth exponent very close to -2 agrees with the theoretical prediction that x does not depend on the opening angle of a linear wedge. Similar behavior has been reported in a previous study [15].

Finally, another interesting feature of the data on the patterned samples regards the location of the crossover from a flatlike to a wedgelike behavior. As expected, the isotherms in Fig. 4 indicate that this crossover moves closer to P_{sat} as the characteristic wedge size increases, in rather good agreement with formula (4). The dependence of such a crossover on the wedge size can be simulated by simply changing the wedge number N_w while keeping the substrate size L constant, since a decrease in N_w implies an increase in the effective wedge size.

It is a pleasure to acknowledge stimulating and clarifying discussions with Professor Andrew Parry. We particularly thank Dr. Marco Bajo for help in the data acquisition, Dr. Paolo Guerriero for the images with the electron microscope, and last, but not least, Dr. Giacomo Torzo for the AFM analysis.

[1] P. Pfeifer, Y. J. Wu, M.W. Cole, and J. Krim, Phys. Rev. Lett. **62**, 1997 (1989).
[2] L. D. Gelb, K. E. Gubbins, R. Radhakrishnan, and M. Sliwinska-Bartkowiak, Rep. Prog. Phys. **62**, 1573 (1999).
[3] See, e.g., C. Bauer and S. Dietrich, Phys. Rev. E **60**, 6919 (1999).
[4] H. Shi, W. B. Tsai, M. D. Garrison, S. Ferrari, and B. D. Ratner, Nature (London) **398**, 593 (1999).
[5] G. M. Whitesides and A. D. Stroock, Phys. Today **42**, No. 6, 42 (2001).
[6] M. Heni and H. Löwen, Phys. Rev. Lett. **85**, 3668 (2000).
[7] C. Rascón and A. O. Parry, Nature (London) **407**, 986 (2000).
[8] E. Cheng and M.W. Cole, Phys. Rev. B **41**, 9650 (1990); M. Napiórkowski, W. Koch, and S. Dietrich, Phys. Rev. A **45**, 5760 (1992).
[9] E. H. Hauge, Phys. Rev. A **46**, 4994 (1992).
[10] K. Rejmer, S. Dietrich, and M. Napiórkowski, Phys. Rev. E **60**, 4027 (1999); A. O. Parry, C. Rascón, and A. J. Wood, Phys. Rev. Lett. **85**, 345 (2000).
[11] See, e.g., J. S. Rowlinson and B. Widom, *Molecular Theory of Capillarity* (Clarendon, Oxford, 1989).
[12] C. Rascón and A. O. Parry, J. Chem. Phys. **112**, 5175 (2000).
[13] The Si pieces have been patterned by Mikromasch, Estonia.
[14] L. D. Landau and E. M. Lifshitz, *Fluid Mechanics* (Pergamon Press, New York, 1959).
[15] L. Bruschi, A. Carlin, and G. Mistura, J. Chem. Phys. **115**, 6200 (2000).
[16] A. O. Parry (private communication).
[17] L.W. Bruch, M.W. Cole, and E. Zaremba, *Physical Adsorption: Forces and Phenomena* (Oxford University Press, New York, 1997).
[18] L. Bruschi and G. Mistura, Phys. Rev. B **61**, 4941 (2000).